Wind Power Ramp Event Forecasting Using a Stochastic Scenario Generation Method

Mingjian Cui, *Student Member, IEEE*, Deping Ke, Yuanzhang Sun, *Senior Member, IEEE*, Di Gan, Jie Zhang, *Member, IEEE*, and Bri-Mathias Hodge, *Member, IEEE*

***Abstract*—Wind power ramp events (WPREs) have received increasing attention in recent years as they have the potential to impact the reliability of power grid operations. In this paper, a novel WPRE forecasting method is proposed which is able to estimate the probability distributions of three important properties of the WPREs. To do so, a neural network (NN) is first proposed to model the wind power generation (WPG) as a stochastic process so that a number of scenarios of the future WPG can be generated (or predicted). Each possible scenario of the future WPG generated in this manner contains the ramping information, and the distributions of the designated WPRE properties can be stochastically derived based on the possible scenarios. Actual wind power data from a wind power plant in the Bonneville Power Administration (BPA) were selected for testing the proposed ramp forecasting method. Results showed that the proposed method effectively forecasted the probability of ramp events.**

***Index Terms*—Genetic algorithm (GA), neural networks (NNs), stochastic process model, stochastic scenario generation, wind power, wind power ramp events (WPREs).**

I. Introduction

THE INTEGRATION of large amounts of wind power, which has variable and uncertain power output, poses challenges in maintaining the power system's traditional levels of reliability [1]. Large fluctuations of wind power in a short time period, such as significant increases or decreases, are known as the wind power ramp events (WPREs) [2]–[4]. WPREs are particularly important in the management and dispatch of wind power. It is sometimes necessary to regulate the output of traditional generators in the power grid to accommodate the substantial fluctuations of wind power, including using grid ancillary services or curtailing the wind turbine output. These actions can have significant economic impacts, and so better forecasting of these events could mitigate the effects; research on WPRE forecasting has shown how this can benefit system operations [5]. Better forecasting of WPREs will help the power system operator (PSO), especially at the economic dispatch timescale.

Ramp events can generally be divided into two basic types based on the direction: up-ramps and down-ramps [6]. Up-ramps commonly have the characteristic that the wind power increases sharply. Strong low pressure air systems (or cyclones), low-level jets, thunderstorms, wind gusts, or similar atmospheric phenomena can induce up-ramps [7]. Likewise, when the wind power drops suddenly or high speed gusts of wind make wind turbines reach cut-out limits (usually 22–25 m/s), wind turbines are shut down [8] to protect themselves from damage. Down-ramps are the reverse physical processes of up-ramps [9], and are generally caused by the same aforementioned meteorological phenomena. Normally, ramp events are parameterized by the following properties: ramp start time, ramp duration, ramp rate, ramp swing, and ramp end time.

Currently, there are two major challenges in forecasting WPREs. The first is that statistical or time series deterministic point prediction methods produce different results after each simulation; these techniques include autoregressive moving average (ARMA) models [10], neural networks (NNs) [11], and support vector machines (SVM) [12]. The second is the challenge in forecasting the ramp characteristics with physical models [13]. These models are generally at a larger geographic scale, and have difficulties in representing the site-specific phenomena, such as local terrain characteristics, which strongly influence WPREs.

Sevlian and Rajagopal [14] defined a family of scoring functions with ramp events definitions and used a dynamic programming recursion technique to detect all the ramp events. They also mentioned that the identified ramps information could be used in forecasting and simulation. Cutler *et al.* [15] forecasted ramp events and evaluated the efficiency of the Wind Power Prediction Tool (WPPT) and the Mesoscale Limited Area Prediction System (MesoLAPS) for ramp event forecasting. However, sudden drops within an interval, causing a premature termination or start for ramp events, were not captured in the analysis. Ramp events in [12] were grouped in classes and the SVM was used to forecast and classify ramp events. This method forecasted ramp events successfully, but its lack of forecasting structure could make it unfavorable for establishing models for future control applications, such as dispatching or unit commitment issues. Bossavy *et al.* [16] used the ramp durations and ramp intensity of the predicted ramp events as additional variables to improve the reliabilities of the quantiles forecasting. It mapped a number of ensemble members forecasting a specific ramp event to a probability of that

Manuscript received June 27, 2014; revised November 21, 2014; accepted December 22, 2014. Date of publication January 23, 2015; date of current version March 18, 2015. This work was supported by the National Basic Research Program of China under Grant 2012CB215101. Paper no. TSTE-00318-2014.

M. Cui, D. Ke, Y. Sun, and D. Gan are with the School of Electrical Engineering, Wuhan University, Wuhan 430072, China (e-mail: mj_cui@whu.edu.cn; kedeping@whu.edu.cn; hubeigandi@whu.edu.cn; yzsun@mail.tsinghua.edu.cn).

J. Zhang and B.-M. Hodge are with the National Renewable Energy Laboratory (NREL), Golden, CO 80401 USA (e-mail: jie.zhang@nrel.gov; bri.mathias.hodge@nrel.gov).

Color versions of one or more of the figures in this paper are available online at http://ieeexplore.ieee.org.

Digital Object Identifier 10.1109/TSTE.2014.2386870

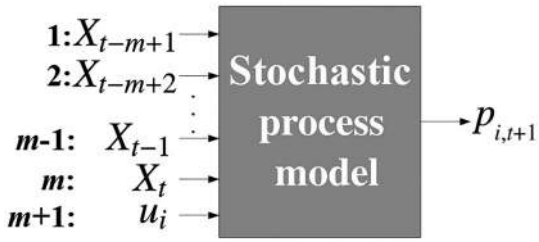

Fig. 1. Novel stochastic process model.

ramp actually occurring, and produced confidence intervals of ramps occurring. But these confidence intervals of ramp events could not be used conveniently in automated dispatching or unit commitment systems. Greaves *et al.* [17] showed a user-friendly way of forecasting up-ramps and down-ramps with uncertain start times and incorporated a numerical weather prediction (NWP) model to reduce the forecasting errors. However, the results relied significantly on improving the NWP forecasts, which, while the subject of much research, was a very difficult problem.

In this paper, a novel probabilistic WPRE forecasting method based on a stochastic process is proposed; the basic process is summarized as follows.

1) NN model is used to simulate the wind power data series as a stochastic process. The inputs and outputs of the NN, as well as the training objective function, are elaborately designed to ensure the acceptable accuracy of the model. A verifying process is also custom-tailored to justify the proposed NN-based stochastic process model.
2) Based on the NN stochastic process model, the possible future scenarios of wind power generation (WPG) can be simulated (or forecasted). The proposed WPRE forecasting approach depends on these forecasted scenarios to extract the important features of the WPREs in a probabilistic manner.

This paper is organized as follows. Section II presents the proposed NN stochastic process model as well as its training and validation methods. Section III introduces the scenario-based WPRE forecasting method. Section IV tests the proposed stochastic process model and the WPRE forecasting method by using actual wind power data. Section V concludes the paper.

II. Stochastic Scenario Generation Method

A. Stochastic Process Model

Compared to most of the conventional approaches, which commonly predict the values of WPG, the method proposed in this paper essentially outputs the occurrence probabilities of all possible values of future WPG. Specifically, it relies on a novel stochastic process model (Fig. 1), which calculates the probabilities based on the available WPG data. In this paper, the WPG is uniformly discretized to M discrete values denoted by u_i ($i = 1, 2, \ldots, M$) over the range of [0, $P_{w\max}$], where $P_{w\max}$ is the maximum wind power output of the wind plant. At any instant in time, the WPG data (measured or predicted) should be among these M possible values. The discretization can accurately reflect the continuous data case if M is selected to be sufficiently large. Moreover, X_t is used to represent the existing

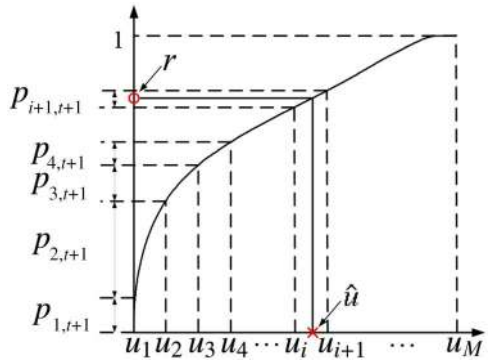

Fig. 2. Schematic diagram for deriving CDF with probability values.

WPG data at the current time instant t while the predicted WPG data at the future time instant $t+1$ is expressed by $\bar{X}_{t+1}$. Therefore, at the time instant t, the inputs of the model (shown in Fig. 1) are the m consecutive WPG data from the time instant $t-m+1$ to t and a possible value of WPG at the time instant $t+1$. The output of the model is the occurrence probability ($P_{i,t+1}$) of the incident that the WPG would be with the value of u_i at the time instant $t+1$. Thus, there are totally M probability values ($P_{1,t+1}, P_{2,t+1}, \ldots, P_{M,t+1}$) sequentially calculated at time instant t by using u_i ($i = 1, 2, \ldots, M$) as the $m+1$ input one after the other while keeping the first m inputs unchanged. After these manipulations, the probability of the WPG being any one of the M values at time instant $t+1$ can be obtained. Specifically, during the calculation process of $P_{1,t+1}, P_{2,t+1}, \ldots, P_{M,t+1}$, a same weights vector is used for the NN. Moreover, these probability values should fulfill the following relationship:

$$\sum_{i=1}^{M} P_{i,t+1} = 1. \tag{1}$$

Once $P_{1,t+1}, P_{2,t+1}, \ldots, P_{M,t+1}$ are known, the cumulative density function (CDF) of $\bar{X}_{t+1}$ can be derived by cumulating these probability values along with $u_1, u_2, \ldots, u_M$ in an ascending order. Such process is schematically depicted in Fig. 2. In particular, all the above calculations are based on one assumption that the occurrence probability can be retrieved by the consecutive WPG data. In other words, the CDF of the WPG at time instant $t+1$ is determined by the last m historical WPG data so that it can be approximately calculated by using the proposed NN-based model. The numerical experiments carried out in the subsequent sections will show the effectiveness of the proposed model through the fundamental mechanism analysis. The general adaption capability of the proposed model is also unique in the literature.

So far, it is noted that with the currently available WPG data, the probability distribution of the WPG at the next time instant can be obtained by the proposed stochastic process model. However, the ultimate objective, in general, is to predict the WPG value so that it can be directly applied in the market or system operations. One straightforward means to do so is to take the expected value according to the obtained CDF of the WPG as the prediction at the next time instant, producing a deterministic estimate. Nevertheless, this method makes much less sense in the context of probabilistic forecasting.

Therefore, in order to entirely mimic the phenomena in the stochastic environment, more meaningful manipulations to produce $\bar{X}_{t+1}$ are proposed as follows: 1) randomly generate a uniformly distributed variable r from the uniform distribution over [0, 1] [18], [19], and locate it in the vertical axis of Fig. 2 (the point identified by a small circle); 2) From that point draw a horizontal line to intersect with the CDF curve; and 3) project the intersection point to the horizontal axis to get a point ($\widehat{u}$) identified by a cross, and if $u_i < \widehat{u} \leq u_{i+1}$, then $\bar{X}_{t+1} = u_{i+1}$. These operations are termed in this paper as the random trial-based realization.

Actually, the physical meaning of generating r from the uniform distribution over [0, 1] is to assist mimicking the random nature of the WPG. At the time instant t, it is believed that the WPG at the time instant $t+1$ will be random. It is noted that even though the probability distribution (CDF) of the WPG at the future time instant $t+1$ is available, its actual value will be unknown at the current time instant t until it really happens in the future. Moreover, supposing that the WPG can repeatedly occur numerous times at the time instant $t+1$, the derived WPG data will have the almost same probability distribution as that calculated by the NN model. For example, before throwing a dice it is exactly known that there will be equal chance to derive any integer between 1 and 6 (in other words, the probability distribution of the result of throwing the dice is known). However, which integer will emerge in practice is impossibly known until the dice is really thrown. Furthermore, if the dice is repeatedly thrown a huge number of times, the actual number of times of any integer emerging should be almost equal to each other. If the CDF of the WPG at the future time instant $t+1$ is available, a WPG data can be accordingly generated by performing the random trial-based realization at the current time instant to mimic the future practical occurrence of the WPG. In particular, generating the number r from the uniform distribution over [0, 1] is the fundamental manipulation of the random trial-based realization. Moreover, it can be understood in this way: if generating r from the uniform distribution over [0, 1] is repeatedly performed numerous times, all the derived r will uniformly distribute between [0, 1]. Then, according to the mapping operation (from p to u), all the obtained WPG data via the mapping can be used to synthesize the CDF as shown in Fig. 2.

B. Scenario Pool Generation

By using the random trial-based realization, the proposed stochastic process model can be further utilized to predict several subsequent steps' WPG data from the current time (e.g., $\bar{X}_{t+1}, \bar{X}_{t+2}, \bar{X}_{t+3}, \ldots, \bar{X}_{t+L}$). These sequential predictions with the length of L constitute a scenario. Indeed, such multiple-step-ahead predictions have been implemented in many deterministic prediction methods [20]–[23]. The length L is chosen with consideration of the time step size to cater to the practical applications, such as the provision of economic spinning reserves or market clearing. Here, a scenario is derived by the following manipulations. Once $\bar{X}_{t+1}$ is generated, it replaces X_t as the m input of the model shown in Fig. 1. X_t replaces X_{t-1} as the $m-1$ input while X_{t-1} replaces X_{t-2} as the $m-2$ input. Such replacements continue propagating until X_{t-m+1} as the first input will be discarded. Then, by keeping these m inputs fixed and setting the $m+1$ input to be $u_1, u_2, \ldots, u_M$, respectively, the CDF of the WPG at the time instant $t+2$ is constructed as described in the previous section. With this CDF, $\bar{X}_{t+2}$ is obtained via the random trial-based realization. Similarly, $\bar{X}_{t+3}$ to $\bar{X}_{t+\mathrm{L}}$ are sequentially calculated by repeating the above manipulations in a recursive manner.

Generally, the classic deterministic forecasting methods are incompetent to accomplish the scenarios prediction, which can be employed for the probabilistic optimal dispatch or market operations. Furthermore, current available probabilistic forecasting methods are generally for one-step-ahead prediction interval which would be limited in the applications requiring multi-step-ahead WPG predictions. However, it should be highlighted here that during each random trial-based realization in the above procedure to produce a scenario, the random number r (uniformly distributed) must be regenerated. Therefore, if this scenario generation procedure is repeated N_s times at the current time instant, N_s scenarios will be produced. These scenarios compose a scenarios pool at the current time instant, and each of them describes one possible WPG evolving trajectory in the future (limited to L steps). From the respect of sampling analysis, the scenarios pool could be regarded as a Monte Carlo simulation of the stochastic process if N_s is selected to be adequately large, and it naturally covers the stochastic characteristics contained in the process model.

It is not difficult to infer that whether the scenarios pool is a good depiction of the measured stochastic process, as well as the credibility of the ramping information extracted from the scenarios (this will be introduced in Section IV), greatly depend on the quality of the stochastic process model. Thus, in the subsequent section, a novel NN-based stochastic process model constructed and trained based on the historical WPG data will be introduced.

III. NN-Based Stochastic Process Model

A. Structure

A three-layer feed-forward NN is employed to play the role of the stochastic process model due to its excellent generality and capability of approximating any nonlinear function [24]. This NN has $m+1$ neurons in the input layer and one neuron in the output layer. The number of neurons in the hidden layer is denoted by N_n. In addition, the sigmoidal function is designated as the activation function while the linear function is used as the output function.

B. Objective Function for Training

Although the proposed NN possesses a fairly common structure, its output is quite unique. Unlike the NN employed in the conventional forecasting approaches which map the wind power or speed (inputs) to the same property of outputs (wind power or speed), this NN outputs the occurrence probability of the wind power in the future time based on the wind power inputs. Thus, the objective function to supervise the training

of such NN is entirely different from that in the commonly used NN predictors. Naturally, it is expected that the WPG data series (the scenario) generated by the NN (the stochastic process model) can fully fit the probabilistic characteristics of the measured stochastic process. To achieve this, the objective function should be properly defined to represent the distinction of the probabilistic characteristics between the NN model and the measured stochastic process. By adjusting the weights of the NN during the training to minimize the objective function, the NN model can enact a good approximation of the measured stochastic process. Here, it should be particularly accentuated which characteristics are numerically extracted from the WPG data: the data generated by the NN model and the historical data of the measured stochastic process. Moreover, the study in this paper considers two probabilistic characteristics which are described in the following.

1) CDF Over the Infinite Time Horizon: It is discussed in Section II that the WPG value at a certain time instant is randomly produced according to its CDF (Fig. 2) at this instant, which is derived based on the stochastic process model and thus the measured WPG data. The CDF varies over time. Additionally, the WPG is actually a random variable with a CDF to measure the occurrence frequency of each value over the infinite time horizon. This CDF is fixed since it is defined with an infinite time horizon. In general, the WPG data must cover a long enough time horizon that it can be used to approximate this CDF [18]. So, a CDF denoted by $F_1(u)$ is constructed depending on the historical WPG data with the large data length of N_h coming from the measured stochastic process. Here, $F_1(u)$ symbolizes the cumulative occurrence probability of the WPG values smaller than u. In the same manner, $F_2(u)$ representing another CDF is derived from the WPG data series (scenario) generated by the NN model. The length L of the scenario used here should also be large enough to encompass sufficient information of the WPG probability distribution over the infinite time horizon. Thus the necessary condition that the NN-based stochastic process model is a sufficient mathematical representation of the measured stochastic process with $F_1(u)$ and $F_2(u)$ as identical as possible, should hold. Accordingly, the following function is defined to identify the distinction between the NN model and the measured stochastic process model from the aspect of the CDF over the infinite time horizon:

$$F = \sum_{i=1}^{M} [F_1(u_i) - F_2(u_i)]^2. \tag{2}$$

2) Second-Order Autocorrelation Function: The CDF mentioned above depicts the overall occurrence frequencies of the WPG values over the infinite time horizon. However, this CDF does not respect the ordinal relationships of the WPG data along the time sequence. When employing the stochastic process model, the occurrence probability of a WPG value at a certain time instant relies on several WPG data occurring in the previous time steps. This definitely manifests the relationship between the fore-and-aft data of the WPG data series. Normally, the sequential relationship of the data series

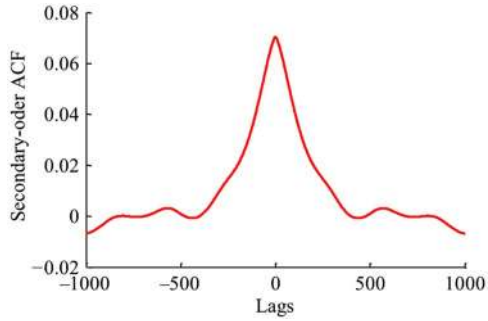

Fig. 3. General profile of a second-order ACF.

is quantitatively measured in statistics by the second-order autocorrelation function (ACF) [25], [26]

$$C_z(\tau) = \frac{1}{N_z} \sum_{t=1}^{N_z} [(Z_t - m_z)(Z_{t+\tau} - m_z)] \tag{3}$$

$$m_z = \frac{1}{N_z} \sum_{t=1}^{N_z} Z_t \tag{4}$$

where Z_t is the data series with the length of N_z and m_z is its statistical mean; τ is the integer to denote the time lag. Fig. 3 illustrates the general profile of a second-order ACF. Therefore, with the historical WPG data, a second order ACF $C_1(\tau)$ is formed to indicate the autocorrelation property of the data. Meanwhile, the scenario (WPG data series) used to generate the CDF in the previous section will produce another second-order ACF $C_2(\tau)$ as a comparison to the $C_1(\tau)$. Thus, the error function defined in the following can intrinsically distinguish the NN model from the measured stochastic process model:

$$C = \sum_{\tau=-N_\tau}^{N_\tau} [C_1(\tau) - C_2(\tau)]^2 \tag{5}$$

where N_τ represents the maximum time lag considered in the construction of the ACFs.

So far, two important probabilistic characteristics (the CDF and the ACF) have been highlighted. In order to train the NN-based stochastic process model to match the measured WPG stochastic process, the objective function for training is defined as follows:

$$f_{\text{obj}} = W_1 C + W_2 F \tag{6}$$

where W_1 and W_2 are the weights of the two error functions. The training process for the NN is to minimize f_{obj} so that $F_2(u)$ and $C_2(\tau)$ can fit $F_1(u)$ and $C_1(\tau)$, respectively. It is important to note that even exactly fitting these two types of functions is not a sufficient condition to ensure the strict concurrence of the NN model and the measured stochastic process. In theory, inclusion of more probabilistic characteristic information in the objective function could enhance the accuracy of the approximation, although the computational time and complexity would be considerably increased. This is also the natural extension of the studies in this paper which will be carried out in the near future. Minimization of the objective function

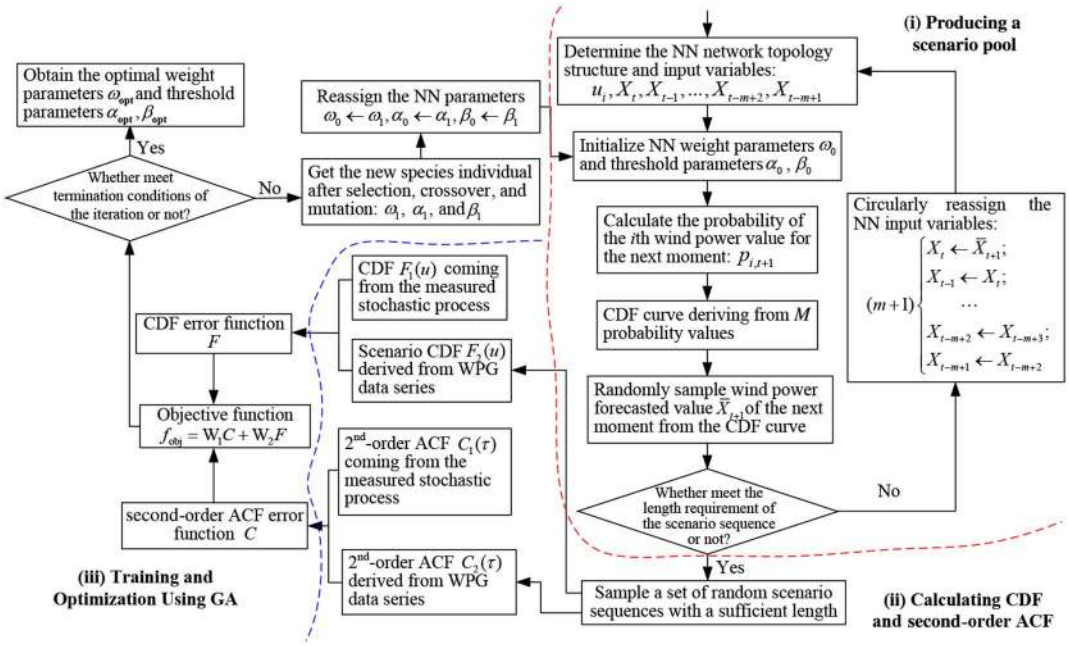

Fig. 4. Flowchart for solving optimal parameters.

used here achieves that sufficiently accurate representation of the measured stochastic process, at least from the viewpoint of the proposed two probabilistic characteristics, should be approximately represented by the NN model. A novel method to verify the effect of the approximation will be introduced in Section III-D, but before that the process of training the NN is demonstrated in the following section.

C. Training Based on GA

The training process is designed to find the optimal weights of the NN so that the objective function is minimized. Because the derivatives of the objective function with respect to the weights cannot be analytically calculated, gradient-based training methods, like the commonly used back-propagation algorithm are not applicable to train the NN. Therefore, the more versatile optimization algorithm GA is employed in this paper for the training. The GA has been recognized as one of the most powerful searching algorithms which possess the capability to find the high-quality (maybe not globally optimal) solution. Generally, the GA with a larger size of population as well as sufficient generations of the evolution tends to find a better solution, although it will cost much more computational time. Moreover, repeating the calculation several times will remarkably avoid finally obtaining an unacceptable solution which may result in large mismatch of the CDFs (and ACFs) synthesized from the simulated WPG data by the NN model and the historical WPG data, respectively. In particular, it will be seen in the subsequent section that the properly configured GA solves the optimization with a quite favorable result even though it may not be the global optima.

The individual in the population of the GA is the weights vector to be optimized, and the GA follows the standard implementation procedure which is not presented due to space limitations. During each iteration (generation), the key is to evaluate the objective function for each individual which ranks its quality among the population. The functions $F_1(u)$ and $C_1(\tau)$ derived from the historical data remain unchanged during the searching. Then, starting with a WPG data series (Fig. 1; the data length is n), a scenario can be generated by the random trial-based realization. In this study, each individual uses the same starting WPG data series obtained by truncating a segment of n consecutive data points from the historical WPG data to produce a scenario. However, it should be noted that all generated scenarios are different due to the use of the random trial-based realization. Therefore, for each individual with a produced scenario, two functions $F_2(u)$ and $C_2(\tau)$ can be synthesized. Finally, with $F_1(u)$, $C_1(\tau)$, $F_2(u)$, and $C_2(\tau)$ the objective function is evaluated by using (2)–(5). The process chart for solving optimal parameters of the NN is shown in Fig. 4. It is made up by three parts: 1) the producing a scenario pool; 2) the calculating CDF and second-order ACF; and 3) the training and optimization using GA.

The proposed NN-based stochastic process model is updated overtime in order to cope with the time-variant characteristics of the system (e.g., changes of the mechanical model of the wind turbine). The newly incoming WPG data will be used to evaluate the approximation effect of the trained NN model by comparing the simulated CDF and ACF with those synthesized from the data. If the weighted error offends the specific limitation, a new-round training (updating) of the NN model will be started with the data set including those fresh data. Moreover, the optimal weights vector calculated in the last round training will be used as one of the individuals in the initialized population of the GA for this updating, so that the overall updating efficiency can be improved. In particular, the updating period of the model in this paper is designed to be one weak. If the computational efficiency can be remarkably enhanced in the

future, much shorter updating period will be viable so as to timely capture the possible small time-scale variations of the system.

In short, the innovation of the paper is to propose a nonlinear model (with the NN structure) to represent the stochastic process of the WPG, the method (employing the GA) to train this model, and finally its applications. First, although the proposed stochastic process model possesses a fairly common NN structure, its output is different from the inputs in property (the inputs are the historical WPG data while the output is the occurrence probability of the WPG being a certain value in the next time instant), which is entirely unlike the NNs employed in the conventional forecasting techniques mapping the wind power or speed (inputs) to the same property of outputs (wind power or speed). Secondly, the NN-based stochastic process model is used to generate the future WPG scenarios (each scenario consists of a series of WPG data) by using the proposed random trial-based realization, which is unique in the wind power forecasting literature. Finally, because unlike the traditional NN-based deterministic wind power forecasting which can straightforwardly construct the objective function for the training, a novel objective function is defined in this paper to train the NN model so that it can sufficiently capture the stochastic nature of the WPG. Specifically, it is expected that the training can drive the CDF and the second-order ACF synthesized from the simulated WPG data (the scenario) via the NN model to be identical to those synthesized from the historical WPG data. So, the objective function for the training is defined based on the CDF and ACF as shown in (2)–(6). After deriving the objective function, it is true that searching the optimal solution (the optimal weights vector) follows the standard GA procedure.

D. Validation of the NN-Based Stochastic Process Model

As indicated at the end of Section III-B, a novel method proposed to validate the NN-based stochastic process model is explained in this section. Besides the training data, another historical WPG data series is used for the verification. Hence, Y_t is used to denote the data at the instant t in the verification data series. With $Y_t, Y_{t+1}, \ldots, Y_{t+n}$ the CDF of the WPG at the instant $t+n+1$ can be constructed according to the method in Section II-A, and it is represented by $F_{\text{ins},t+n+1}(u)$. Given a confidence level $\eta (0 < \eta \leq 1)$, the corresponding quantile is obtained by taking the inverse function of $F_{\text{ins},t+n+1}(u)$ as follows:

$$u_{t+n+1}^{(\eta)} = F_{\text{inst},t+n+1}^{-1}(\eta). \tag{7}$$

In other words, the WPG data at the instant $t+n+1$ should be randomly located within the confidence interval $[0,\ u_{t+n+1}^{(\eta)}]$ with the confidence level η. It is noted that the inputs $(Y_t, Y_{t+1}, \ldots, Y_{t+n})$ to the NN model at any instant t are the real WPG data, which means that the CDF of the WPG constructed at any instant is a deterministic function. Generating the WPG data according to the CDF at any instant via the random trial-based realization should be mutually independent. By setting $t = 1, 2, \ldots, N_v$, respectively, N_v WPG data will be generated in that way. Thus, as long as the number of the data points (N_v) is large enough, the probability of the points being located within their corresponding confidence intervals is η.

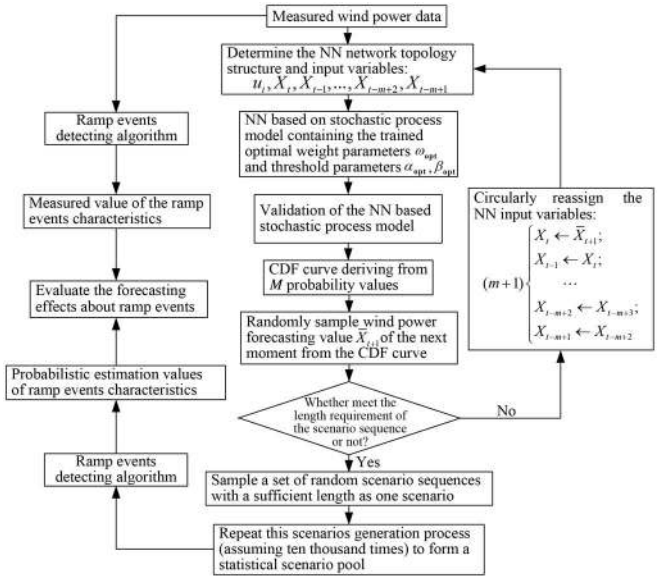

Fig. 5. Holistic procedure of the proposed method with optimization, validation, and evaluation.

In the light of above analysis, a flag variable $s_{t+n+1}^{(\eta)}$ is defined to indicate whether the measured WPG data Y_{t+n+1} at the instant $t+n+1$ is covered by the confidence interval or not, by comparing it with $u_{t+n+1}^{(\eta)}$

$$s_{t+n+1}^{(\eta)} = \begin{cases} 1, & \text{if } Y_{t+n+1} \leq u_{t+n+1}^{(\eta)} \\ 0, & \text{if } Y_{t+n+1} > u_{t+n+1}^{(\eta)}. \end{cases} \tag{8}$$

As t varies from 1 to N_v, N_c is the number of instances where the measured WPG data reside within the confidence interval associated with η

$$N_c = \sum_{t=1}^{N_z} s_{t+n+1}^{(\eta)}. \tag{9}$$

Therefore, if the NN model is the feasible approximation of the measured stochastic process, the number N_c/N_v should be quite close to η. To ensure the adequacy of the verification, the comparisons between N_c/N_v and η are conducted with different η values. The flowchart including optimization, validation, and evaluation is shown in Fig. 5.

IV. Experimental Results

The proposed NN-based stochastic process model is verified and then applied to the probabilistic forecasting of WPREs in this section. The WPG data used in this paper is from the Bonneville Power Administration (BPA). The data are sampled every 15 min from January 1, 2005 to December 31, 2006 (the total number of samples is 70 080) and is used as the training data of the NN model. The verification process uses the historical WPG data recorded from January 1, 2005 to April 14, 2005,

and the number of test data points is 10 000. The number of the consecutive WPG data as the inputs to the NN model is set to be 5 ($m = 5$). The length of one scenario is assumed 70 000 (about 730 days). With the additional input denoting the possible value of the WPG at the next time instant, the total number of the inputs of the NN model is 6. There are eight neurons in the hidden layer. Thus, total 65 ($= 6 \times 8 + 8 \times 1 + 8 + 1$) weight coefficients are optimized during the training. The GA is employed to train the NN model with a population size of 195 individuals (NNs) and the maximum iterative generation of 1000. Specifically, the weights in the objective function (6) are chosen to be $W_1 = W_2 = 1$. All calculations in this section are performed on a desktop with an Intel i7-2640M CPU at 2.80 GHz and with 3 GB RAM.

A. Training Results and Verification

It takes around 16 h (672 generations) for the GA to decrease the objective function to a value smaller than the specified tolerance. The calculation of the proposed NN model based on the GA is computationally expensive. Although it has been scheduled that the computational efficiency is not the primary concern at the current stage (paper) of such content-rich research topic, this is undoubtedly a key issue deserving dedicated studies in the future. Some attempts can be made toward the following directions to reduce the time cost of training the proposed NN model. 1) An advanced filtering technique will be proposed to rapidly identify a small number of individuals which are fairly possible to be the high-quality solutions among the population in each generation; then, only these individuals will undergo the time-consuming accurate evaluation (calculate the fitness function), which can thus save considerable time without deteriorating too much searching quality in comparison to the standard GA accurately evaluating all individuals in each generation. (2) Because the GA is employed, an advanced parallel computing platform can be used to significantly reduce the computation time.

The evolutions of the CDF and the ACF related to the NN-based stochastic process model during the training phases are shown in Fig. 6. It is seen that the optimization by the GA can effectively drive them to gradually approach their counterparts derived from the historical WPG data. Moreover, the fitting of these two functions is quite accurate when the NN model uses the final optimized weighting coefficients. This implies that the NN model can precisely mimic the measured stochastic process, at least in the sense of a consistent CDF and ACF.

According to the method proposed in Section III-D, given a value of η, the corresponding N_c/N_v can be calculated from the WPG data series (scenario) generated by the NN model. The parameter N_v is the number of data points, and N_c is the number of instances where the measured WPG data reside within the confidence interval associated with η. Different N_c/N_v ratios can be derived with multiple η values. The corresponding points (η, N_c/N_v) are plotted in Fig. 7 to visually show the relationship between N_c/N_v and η which is calculated based on the NN model (these points are identified by the circles). For the ideal case, the NN model would be an exact representation of the measured stochastic process. If the length of the historical

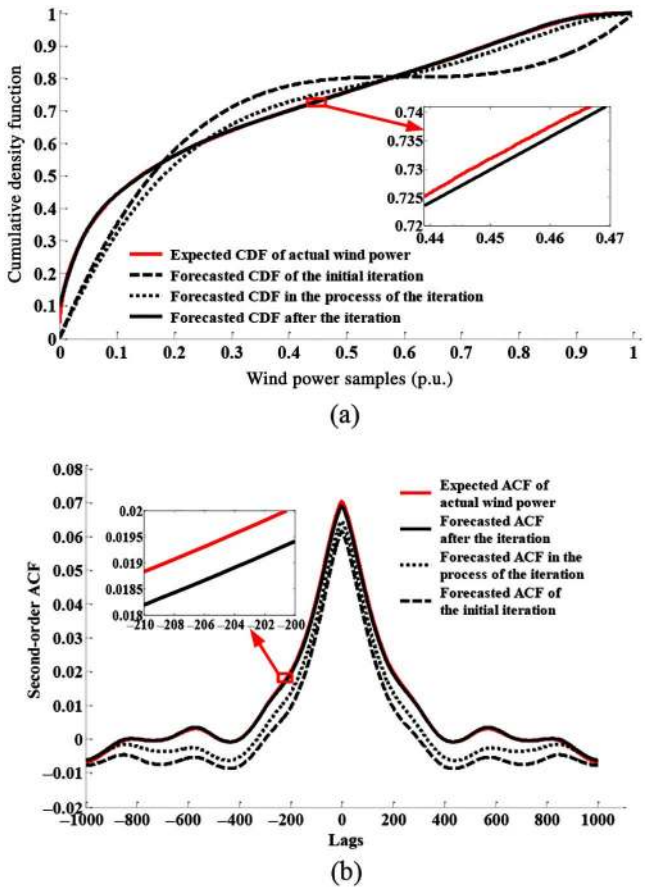

Fig. 6. Iterative schemes of the CDF and second-order ACF. (a) CDF iterative schemes. (b) ACF iterative schemes.

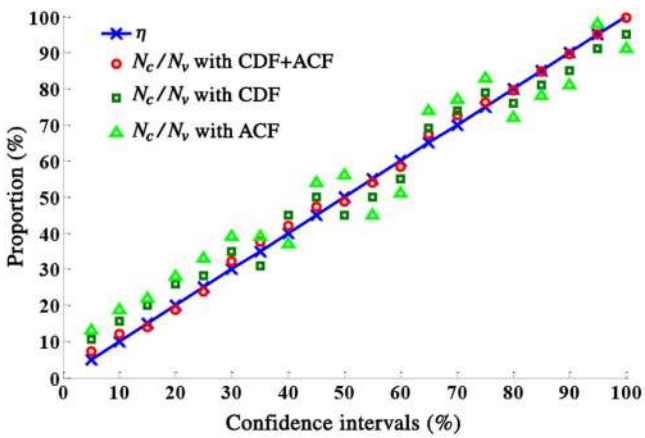

Fig. 7. Statistical results of η and N_c/N_v index.

WPG data used for the verification is infinitely large, N_c/N_v would be strictly equal to η ($N_c/N_v = \eta$) which is shown by the blue line in Fig. 7.

Validation of the proposed NN-based method should be performed based on the comparisons of statistical characteristics between the predicted WPG data set by the NN model and the real WPG data set. This is actually quite different from the manner used to evaluate the performance of the classic forecasting methods by directly comparing the real WPG data and their predictions. In the context of the proposed probabilistic

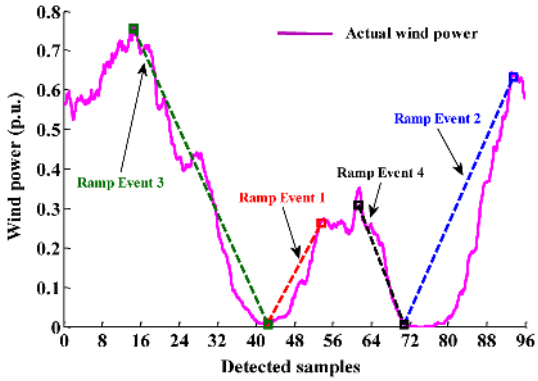

Fig. 8. Detected actual WPREs during a certain period.

forecasting method in this paper, it is important to validate the model by a fairly long WPG data set, since the statistical characteristics can be only reliably extracted from a data set with a sufficiently large size. In the exhibited application, the NN model is employed to predict the WPG (scenarios) corresponding to a single day which is generally the planning period of the power system dispatching. However, it can be observed that a huge number of the WPG data is utilized to verify the proposed stochastic process model in Fig. 7. A novel method is used to identify the consistence of the statistical characteristics derived, respectively, from the NN prediction and the historical data.

In Fig. 7, the circles are found to closely locate around the blue line (representing the ideal case), illustrating the accuracy of the NN-based stochastic process. Moreover, the errors between the percentage of N_c/N_v and the confidence interval associated with η. It is visually observed that the red circles (by both CDF and ACF) are closer to the blue line (the confidence interval η line) than the dark green boxes (only by CDF) and the green triangles (only by ACF).

B. Distribution of Single Characteristic Experiment

Detected ramp events based on the scenarios pool introduced in Fig. 8 are taken as the reference case, and the length of each scenario is set to be 96 time points (1 day). The detecting algorithm proposed in [14] and [27] is used to identify all of the ramp events (up-ramps and down-ramps). Statistical analysis is conducted with a large amount of forecasted characteristics data. The NN model weights are compared with different objective functions: 1) the single CDF; 2) the single ACF; and 3) the combination CDF and ACF. Statistical results of three ramp events features (ramp start time, ramp duration, and ramp swing) are shown in Fig. 9.

In Fig. 8, there are four ramp events identified by the detecting algorithm. The specific features of these WPREs are listed in Table I.

Fig. 9 illustrates that the proposed method using the combined objective function (CDF + ACF) is more accurate than the other two methods only using the CDF or the ACF objective function. This is because the CDF + ACF objective function considers not only the wind power distribution characteristics of historical wind power data but also the autocorrelation of the sequence. The reason that second-order features are more

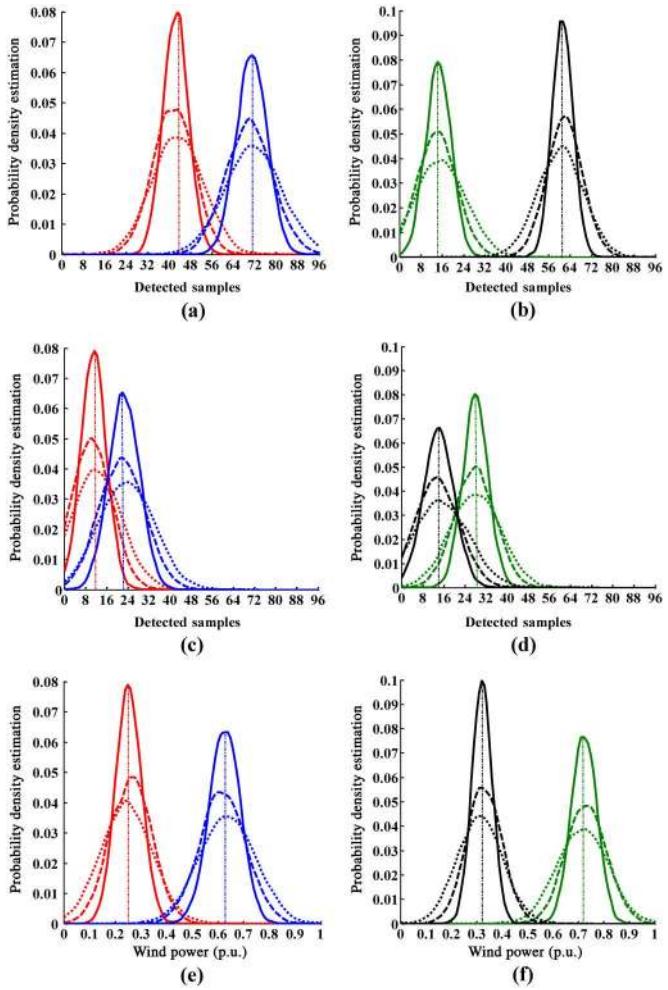

Fig. 9. Probability density estimation charts of the characteristics. Solid lines, dashed lines, and dotted lines represent using the CDF + ACF, CDF, and second-order ACF objective functions, respectively. The red line is ramp Event 1. The blue line is ramp Event 2. The green line is ramp Event 3. The black line is ramp Event 4. (a), (c), and (e) are the three estimated ramp event features (i.e., start time, duration, and swing) for up-ramps. (b), (d), and (f) are the features for down-ramps.

TABLE I
SPECIFIC FEATURES OF THE FOUR RAMP EVENTS

Ramp events	Start time (point/min)	Duration (point/min)	Swing (p.u.)
Event 1	43rd/645	11/165	0.2625
Event 2	71st/1065	23/345	0.628
Event 3	15th/225	28/420	0.7305
Event 4	61st/915	10/150	0.3035

important is that each characteristic of ramp events is closely related to the temporality of actual wind power data. During the iterative process of forecasting output data, second-order features can make sorting features of output data fully conform to that of actual wind power data and guarantee the strong correlations between them. It is seen that probability density estimation values calculated by the three methods are different, which means that statistical results of the CDF + ACF objective functions are more concentrated and have more statistical significance.

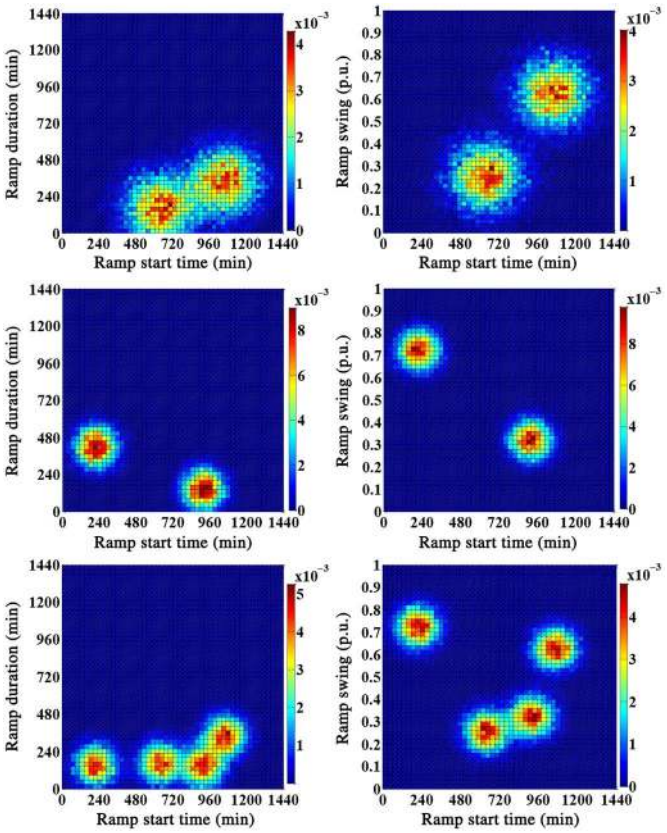

Fig. 10. (Left) Joint distribution of ramp start time and ramp duration for up-ramps, down-ramps, and all the events. (Right) Joint distribution of ramp start time and ramp swing for up-ramps, down-ramps, and all the events.

C. Joint Distribution Experiments of Ramp Start Time With Ramp Duration and Ramp Swing

Based on the forecasted information of ramp event characteristics, the degree of correlation among them can be analyzed. Joint distributions of these characteristics are shown in Fig. 10.

Fig. 10 shows that the correlation degree of the up-ramps characteristics is lower than that of the down-ramps characteristics. This is because the joint distributions of the up-ramps are relatively scattered while that of the down-ramps are relatively concentrated, which raises the degree of correlation. Although ramp events may happen at any moment, the ramp duration does not exceed 600 min (10 h) during the period of 1 day. Moreover, when a ramp event occurs, the occurrence possibility of the next ramp event is higher. This phenomenon needs more attention from PSOs. It is also observed that up and down ramp events start at different times and the corresponding ramp swings are also different. This information could be utilized by the system operator to design more efficient ramp mitigation options, such as dynamic reserve levels.

D. Generalization Capability of the Proposed NN Model and Comparison With Conventional WPG Forecasting Method

In this section, the training data set will be different from the verification data set so as to check the generalization capability of the proposed NN model. Specifically, the training data of the NN model are sampled every 1 min from January 1, 2005 to December 31, 2005, while the verification process uses the new WPG data recorded from January 1, 2006 to December 31, 2006 as the test data set. By using the method introduced in Section III-D for the verification, Fig. 11 is drawn based on the test data set. It is seen that although the test data is excluded during the training process, the proposed NN-based stochastic process model can perform rather acceptably (N_c/N_v closely approaches η) as well to reflect the probabilistic characteristics of the test data set, which proves its generalization capability.

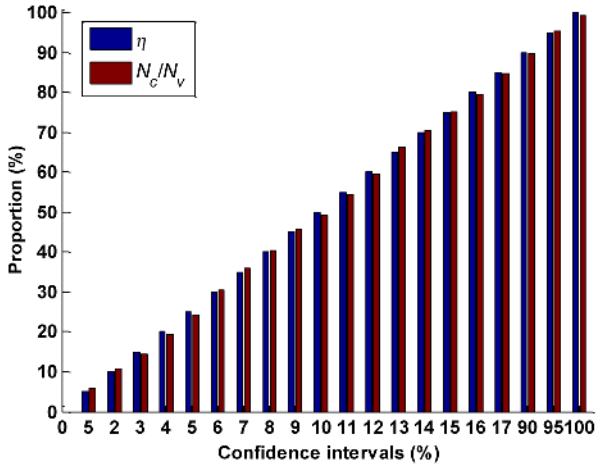

Fig. 11. Comparison of statistical results N_c/N_v and η in the test data set.

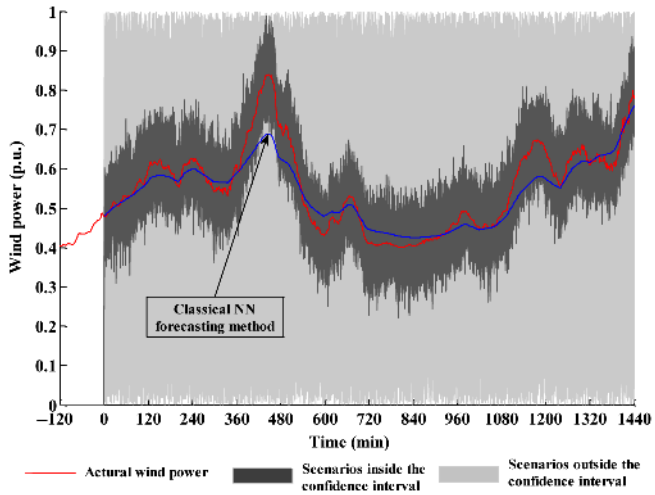

Fig. 12. Comparison of the proposed scenarios prediction method with the classic deterministic forecasting method.

An NN-based deterministic forecasting method [28] is employed as a comparison to the proposed scenarios prediction method. Specifically, at the beginning of the day January 1, 2006, the scenarios pool is predicted by using the method introduced in Section II-B based on the historical data before that day; and 10 000 scenarios are generated for the day January 1, 2006. Then, all these scenarios are plotted in Fig. 12, and the dark gray band represents the most concentrated area which consists of around 90% of all the scenarios. Furthermore, the actual WPG data in that day are also depicted in this figure, and it is observed that coincidently the curve standing for the actual WPG is entirely covered by the dark gray band. However, it

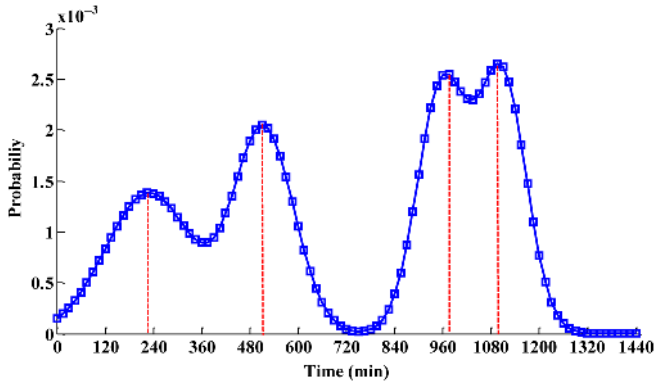

Fig. 13. Distribution of all the start times in the next day (1440 min).

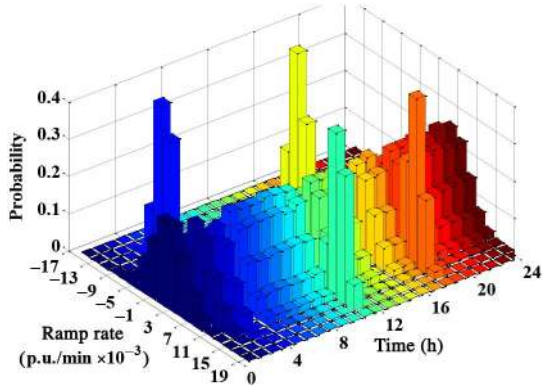

Fig. 14. Probabilities of ramp rates in the next 24 h (1 day).

should be noted that this may not be always the case if the same operations as above are performed for another day, because there is still around 10% of the scenarios escaping from the band. Apparently, these scenarios can be applied for the probabilistic day-ahead dispatching applications in power systems. Furthermore, since the ramp events can be extracted in one predicted scenario, the probability distribution of the ramp events in the next day can be predicted, just as done in the previous sections. In contrast, an evolving curve of the WPG in that day is predicted by the NN-based deterministic method in such feedback manner; the prediction at the current point will be used as one of the inputs (by discarding the oldest input) to produce the prediction at next point. However, it is noted that the derived curve significantly deviates from the actual one, which is not displayed in Fig. 12. Then, the point-by-point prediction is performed by this deterministic method with the actual WPG data as the inputs at each point. It is seen in Fig. 12 that the prediction (the blue cure) can accurately track the actual value point-by-point, which is suitable for the one-point-ahead dispatching or planning applications. Nevertheless, the deterministic NN is not capable of producing the credible WPG scenarios of the next whole day which are the primary outcomes of the proposed NN-based stochastic process model in this paper.

E. Utilizing Forecasted Ramp Events Statistics in Power System Analysis

After generating all the predicted scenarios (10 000 scenarios of the next whole day each with 1440 min), it should be considered how to make this information more practically useful for the PSOs experiencing high penetrations of wind power. Moreover, modeling the impact of ramp events on power system operational costs should be considered, with mitigating ramp events by using improved wind turbine controls as one possibility. PSOs need to know when to limit the ramp rate of wind turbines and coordinate the ramp rate of the power system. Thus, all the start times of ramp events detected by using the L1-trending with sliding window algorithm [14], [27] and the corresponding probabilities are shown in Fig. 13. PSOs also need to decide the rates of wind power ramp events which should be tolerated and the traditional units (especially the thermal-power units and hydro-power units) that can provide compensating power. Therefore, all the ramp events occurring at different time of the day and their values with the corresponding probabilities are depicted in Fig. 14. In order to supply the specific forecasting information to PSOs for the application in unit commitment or dispatching, the values with the maximum probability are enumerated in Table II.

TABLE II
SPECIFIC MAXIMUM PROBABILITY RESULTS IN THE NEXT 24 H

Time (h)	Value (p.u./min)	Probability (%)	Time (h)	Value (p.u./min)	Probability (%)
1	0.001	22.91	13	0.002	22.08
2	0.003	24.08	14	–0.003	23.18
3	0.005	23.33	**15**	**–0.007**	**46.30**
4	**–0.009**	**43.67**	16	0.001	22.34
5	0.003	22.90	17	0.003	24.09
6	–0.003	23.38	**18**	**0.011**	**45.37**
7	0.002	21.36	19	–0.002	23.47
8	–0.001	23.94	20	0.003	21.46
9	0.003	22.68	21	0.001	24.12
10	–0.002	23.15	22	0.002	22.96
11	**0.011**	**44.41**	23	–0.003	24.52
12	0.003	23.27	24	0.001	22.43

Fig. 13 illustrates four maximum probabilities at 210, 520, 990, and 1110 min, respectively, which require PSOs to pay more attention to these time points than other time points. To identify the direction of ramps, an alternative visualization is provided in Fig. 14.

Fig. 14 and Table II provide more specific forecasting information. For example, Table II illustrates that there is a 43.67% chance of a down ramp (with a negative value 0.009 p.u./min) at the 4th hour. Meanwhile there are, respectively, 44.41%, 46.30%, and 45.37% chances of occurring the other three ramps (with 0.011 p.u./min up-ramp at the 11th hour, 0.007 p.u./min down-ramp at the 15th hour, and 0.011 p.u./min up-ramp at the 18th hour). This information (the maximum probability $P_{\max}$ and the ramp rate R_v) can be utilized in the unit commitment, especially in the stochastic unit commitment problem with chance constraints [29]–[31], and scheduling problems [32] to reduce the cost caused by WPREs.

V. CONCLUSION

In this paper, a novel probabilistic WPRE forecasting method was proposed. First, an NN model was developed to generate possible WPG future scenarios, which effectively approximated

the measured WPG stochastic process. In particular, employing the CDF- and ACF-based objective function to train the NN significantly improved the accuracy of the approximation process. Moreover, a scenario pool was produced via a novel random trial-based realization. Subsequently, the focused properties of the WPREs were extracted from each scenario and their probabilistic distributions were stochastically derived. Comparisons carried out based on real wind power data were shown that the proposed NN model could quite satisfactorily simulate the measured WPG stochastic process model. Furthermore, the proposed WPREs forecasting method provided statistical information regarding the ramping events, which was uniquely useful for power systems unit commitment and dispatch with significant penetrations of the wind power.

ACKNOWLEDGMENT

The authors would like to thank the anonymous reviewers for their constructive suggestions to this research.

REFERENCES

[1] P. Sorensen *et al.*, "Power fluctuations from large wind farms," *IEEE Trans. Power Syst.*, vol. 22, no. 3, pp. 958–965, Aug. 2007.

[2] H. Zheng and A. Kusiak, "Prediction of wind farm power ramp rates: A data-mining approach," *J. Solar Energy Eng.*, vol. 131, no. 3, pp. 031011–031018, Jul. 2009.

[3] N. Navid and G. Rosenwald, "Market solutions for managing ramp flexibility with high penetration of renewable resource," *IEEE Trans. Sustain. Energy*, vol. 3, no. 4, pp. 784–790, Oct. 2012.

[4] AWS Truewind. (2008, Jun. 25). *AWS Truewind's Final Report for the Alberta Forecasting Pilot Project* [Online]. Available: http://www.aeso.ca/downloads/Al-berta_PP_Final_Rep-ort_AWST_Jun25.pdf

[5] C. Kamath, "Understanding wind ramp events through analysis of historical data," in *Proc. Transm. Distrib. Conf. Expo.*, New Orleans, LA, USA, 2010, pp. 1–6.

[6] Y. F. Wang and N. Chen, "Impact of WRIG and DFIG wind generation ramping down on independent power systems," in *Proc. IEEE PES/IAS Sustain. Alternative Energy(SAE)*, Valencia, Spain, 2009, pp. 1–7.

[7] C. Kamath, "Associating weather conditions with ramp events in wind power generation," in *Proc. Power Syst. Conf. Expo. (PSCE)*, Phoenix, AZ, USA, 2011, pp. 1–8.

[8] J. Freedman, M. Markus, and R. Penc. (2008, Jan. 28). *Analysis of West Texas Wind Plant Ramp-Up and Ramp-Down Events* [Online]. Available: http://interchange.puc.state.tx.us/WebApp/Interchange/Documents/33672_1014_580034.pdf

[9] C. Ferreira, J. Gama, L. Matias, A. Botterud, and J. Wang, "A survey on wind power RAMP forecasting," Argonne National Lab. (ANL), DuPage County, IL, USA, Tech. Rep. ANL/DIS-10-13, Dec. 2010.

[10] C. Barber *et al.*, *Auto-Regressive HMM Inference With Incomplete Data for Short-Horizon Wind Forecasting*. Cambridge, MA, USA: MIT Press, 2010, pp. 136–144.

[11] C. Gallego, A. Costa, and A. Cuerva, "Improving short-term forecasting during ramp events by means of regime-switching artificial neural networks," in *Proc. 10th EMS Annu. Meeting; Proc. 8th Eur. Conf. Appl. Climatol. (ECAC)*, Zürich, Switzerland, 2010, pp. 55–58.

[12] H. Zareipour, D. Huang, and W. Rosehart, "Wind power ramp events classification and forecasting: A data mining approach," in *Proc. IEEE Power Energy Soc. Gen. Meeting*, San Diego, CA, USA, 2011, pp. 1–3.

[13] K. T. Bradford, R. L. Carpenter, and B. L. Shaw, "Forecasting Southern Plains wind ramp events using the WRF model at 3-km," in *Proc. Amer. Meteorol. Soc. (AMS) Student Conf.*, Atlanta, GA, USA, 2010, pp. 1–10.

[14] R. Sevlian and R. Rajagopal, "Detection and statistics of wind power ramps," *IEEE Trans. Power Syst.*, vol. 28, no. 4, pp. 3610–3620, Nov. 2013.

[15] N. Cutler, M. Kay, K. Jacka, and T. S. Nielsen, "Detecting categorizing and forecasting large ramps in wind farm power output using meteorological observations and WPPT," *Wind Energy*, vol. 10, no. 5, pp. 453–470, Sep. 2007.

[16] A. Bossavy, R. Girard, and G. Kariniotakis, "Forecasting uncertainty related to ramps of wind power production," in *Proc. Eur. Wind Energy Conf. Exhib. (EWEC)*, Warsaw, Poland, 2010, pp. 1–9.

[17] B. Greaves, J. Collins, J. Parkes, and A. Tindal, "Temporal forecast uncertainty for ramp events," *Wind Eng.*, vol. 33, no. 4, pp. 309–320, 2009.

[18] X. Y. Ma, Y. Z. Sun, and H. L. Fang, "Scenario generation of wind power based on statistical uncertainty and variability," *IEEE Trans. Sustain. Energy*, vol. 4, no. 4, pp. 894–904, Oct. 2013.

[19] D. Villanueva, A. Feijoo, and J. L. Pazos, "Simulation of correlated wind speed data for economic dispatch evaluation," *IEEE Trans. Sustain. Energy*, vol. 3, no. 1, pp. 142–149, Jan. 2012.

[20] M. Khalid and A. V. Savkin, "A method for short term wind power prediction with multiple observation points," *IEEE Trans. Power Syst.*, vol. 27, no. 2, pp. 579–586, May 2012.

[21] K. Bhaskar and S. N. Singh, "AWNN assisted wind power forecasting using feed-forward neural network," *IEEE Trans. Sustain. Energy*, vol. 3, no. 2, pp. 306–315, Apr. 2012.

[22] J. Zeng and W. Qiao, "Short-term wind power prediction using a wavelet support vector machine," *IEEE Trans. Sustain. Energy*, vol. 3, no. 2, pp. 255–264, Apr. 2012.

[23] N. Amjady, F. Keynia, and H. Zareipour, "Wind power prediction by a new forecast engine composed of modified hybrid neural network and enhanced particle swarm optimization," *IEEE Trans. Sustain. Energy*, vol. 2, no. 3, pp. 265–276, Jul. 2011.

[24] G. Sideratos and N. D. Hatziargyriou, "Probabilistic wind power forecasting using radial basis function neural networks," *IEEE Trans. Power Syst.*, vol. 27, no. 4, pp. 1788–1796, Nov. 2012.

[25] J. M. Sexauer, "Development of probabilistic load flow for voltage quality analysis in the presence of distributed generation," M.S. thesis, Dept. Electrical Engineering and Computer Science, Colorado School of Mines, Golden, CO, USA, 2012.

[26] J. F. Cardoso, "Source separation using higher order moments," in *Proc. Int. Conf. Acoust. Speech Signal Process.*, Glasgow, Scotland, U.K., 1989, pp. 2109–2112.

[27] R. Sevlian and R. Rajagopal, "Wind power ramps: Detection and statistics," in *Proc. IEEE Power Energy Soc. Gen. Meeting*, San Diego, CA, USA, 2012, pp. 1–8.

[28] G. N. Kariniotakis, G. S. Stavrakakis, and E. F. Nogaret, "Wind power forecasting using advanced neural networks models," *IEEE Trans. Energy Convers.*, vol. 11, no. 4, pp. 762–767, Dec. 1996.

[29] Q. P. Zheng, J. Wang, and A. L. Liu, "Stochastic optimization for unit commitment—A review," *IEEE Trans. Power Syst.*, pp. 1–12, Sep. 2014, to be published.

[30] Q. Wang, Y. Guan, and J. Wang, "A chance-constrained two-stage stochastic program for unit commitment with uncertain wind power output," *IEEE Trans. Power Syst.*, vol. 27, no. 1, pp. 206–215, Feb. 2012.

[31] U. A. Ozturk, M. Mazumdar, and B. A. Norman, "A solution to the stochastic unit commitment problem using chance constrained programming," *IEEE Trans. Power Syst.*, vol. 19, no. 3, pp. 1589–1598, Aug. 2004.

[32] H. Wu, M. Shahidehpour, Z. Li, and W. Tian, "Chance-constrained day-ahead scheduling in stochastic power system operation," *IEEE Trans. Power Syst.*, vol. 29, no. 4, pp. 1583–1591, Jul. 2014.

Mingjian Cui (S'12) received the B.E. degree in electrical engineering and automation from Wuhan University, Wuhan, China, in 2010, where he is currently pursuing the Ph.D. degree in electrical engineering.

Currently, he is a Visiting Scholar with the Transmission and Grid Integration Group (TGIG), National Renewable Energy Laboratory (NREL), Golden, CO, USA. His research interests include wind power ramp events forecasting, power system control, and big data analytics.

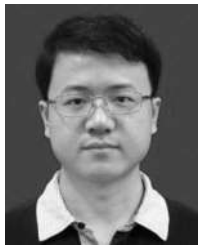

Deping Ke received the B.S. and M.S. degrees in electrical engineering from Huazhong University of Science and Technology, Wuhan, China, in 2005 and 2007, respectively, and the Ph.D. degree in electrical engineering from Hong Kong Polytechnic University, Hong Kong, China, in 2012.

Currently, he is a Lecturer with the School of Electrical Engineering, Wuhan University, Wuhan, China. His research interests include power system dynamics and control.

Yuanzhang Sun (M'99–SM'01) received the B.S. degree in hydro and electrical engineering from Wuhan University, Wuhan, China, in 1987, the M.S. degree from the Electric Power Research Institute (EPRI), Beijing, China, in 1982, and the Ph.D. degree in electrical engineering from Tsinghua University, Beijing, China, in 1988.

Currently, he is a Professor with the School of Electrical Engineering, Wuhan University, and a Chair Professor with the Department of Electrical Engineering and Vice Director of the State Key Laboratory of Power System Control and Simulation, Tsinghua University. His research interests include the areas of power system dynamics and control, wind power, voltage stability and control, and reliability.

Di Gan received the B.E. degree in electrical engineering and automation from Wuhan University, Wuhan, China, in 2013, where he is currently pursuing the Master's degree in electrical engineering.

His research interest includes wind power forecasting.

Jie Zhang (M'13) received the B.S. and M.S. degrees in mechanical engineering from Huazhong University of Science and Technology, Wuhan, China, in 2006 and 2008, respectively, and the Ph.D. degree in mechanical engineering from Rensselaer Polytechnic Institute, Troy, NY, USA, in 2012.

He is currently a Research Engineer with the Transmission and Grid Integration Group (TGIG), National Renewable Energy Laboratory (NREL), Golden, CO, USA. His research interests include multidisciplinary design optimization, complex engineered systems, big data analytics, wind energy, renewable integration, and energy systems modeling and simulation.

Bri-Mathias Hodge (M'10) received the B.S. degree in chemical engineering from Carnegie Mellon University, Pittsburgh, PA, USA, in 2004, the M.S. degree from the Process Design and Systems Engineering Laboratory of Åbo Akademi, Turku, Finland, in 2005, and the Ph.D. degree in chemical engineering from Purdue University, West Lafayette, IN, USA, in 2010.

Currently, he is a Section Supervisor of System Planning and Reliability with the Transmission and Grid Integration Group (TGIG) and a Senior Engineer with the National Renewable Energy Laboratory (NREL), Golden, CO, USA. His research interests include energy systems modeling, simulation, optimization, and wind power forecasting.